



HAL
open science

Highlighting real capacitor behavior in liquid ammonia of passivated n-InP by thin Polyphosphazene film

Gianluca Visagli, Arnaud Etcheberry, Anne-Marie Gonçalves

► To cite this version:

Gianluca Visagli, Arnaud Etcheberry, Anne-Marie Gonçalves. Highlighting real capacitor behavior in liquid ammonia of passivated n-InP by thin Polyphosphazene film. *Electrochemistry Communications*, 2025, 176, pp.107935. <10.1016/j.elecom.2025.107935>. <hal-05060175>

HAL Id: hal-05060175

<https://hal.science/hal-05060175v1>

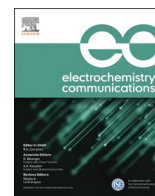
Submitted on 9 May 2025

HAL is a multi-disciplinary open access archive for the deposit and dissemination of scientific research documents, whether they are published or not. The documents may come from teaching and research institutions in France or abroad, or from public or private research centers.

L'archive ouverte pluridisciplinaire HAL, est destinée au dépôt et à la diffusion de documents scientifiques de niveau recherche, publiés ou non, émanant des établissements d'enseignement et de recherche français ou étrangers, des laboratoires publics ou privés.



Distributed under a Creative Commons CC BY 4.0 - Attribution - International License



Highlighting real capacitor behavior in liquid ammonia of passivated n-InP by thin Polyphosphazene film

Gianluca Visagli^{*}, Arnaud Etcheberry, Anne-Marie Gonçalves

Université Paris-Saclay, UVSQ, CNRS, UMR 8180 Institut Lavoisier de Versailles, 78035 Versailles Cedex, France

ARTICLE INFO

Keywords:

InP
Ammonia
Semiconductor passivation
Capacitor-like behavior
Impedance
Cycle voltammetry

ABSTRACT

Semiconductor/liquid junctions exhibit distinctive electrochemical behaviors. This study investigates the passivation of lightly doped (10^{15} cm^{-3}) n-type indium phosphide (n-InP) in liquid ammonia. Under photoanodic conditions, a Polyphosphazene (PPP) film forms on the InP surface. The formation of PPP ultra-thin film was confirmed through X-ray photoelectron spectroscopy. Cyclic voltammetry revealed a progressive positive shift in the onset potential for photocurrent, indicating successful progressive passivation. Capacitance–voltage measurements showed a constant capacitance ($\approx 1.3 \mu\text{F}\cdot\text{cm}^{-2}$) over 400 mV after passivation, signifying the formation of a stable capacitor-like structure at the interface in a large potential domain. Cyclic voltammograms acquired at different scan rates demonstrated that the current was proportional to the scan rate, confirming the capacitive nature of the InP/PPP interface. The same interface capacitance was also quantified from the slope of the linear fit between the current and scan rate, showing that the PPP film acts as a dielectric layer with a fixed capacitance. This capacitor-like behavior leads the semiconductor in accumulation configuration from open circuit potential to lower potentials. To balance the electrical charges, the PPP should be positively charged in this range of potentials. The capacitance was used to determine the relative dielectric constant of the PPP film, which was found to be approximately 6.9. This value is consistent with that of polymeric materials exhibiting good insulating properties, further supporting the effective dielectric behavior of the PPP layer. This capacitor-like behavior alters the electrochemical response and stability of the InP/ NH_3 Liq. interface, underscoring its potential for innovative electrochemical applications.

1. Introduction

Semiconductor (SC)/liquid junctions exhibit highly distinctive behaviors, giving rise to original and specific electrochemical concepts compared to metals [1–4]. Semiconductor electrochemistry often involves surface chemical modifications driven by anodic or cathodic processes, which are highly dependent on the semiconductor's nature and the electrolyte's composition. Among the various liquid junctions, the SC/liquid ammonia interface demonstrates unique electrochemical reactions [5–8], linked to the remarkable properties of liquid ammonia (NH_3 Liq.) including low viscosity, low dielectric constant, and an exceptionally broad alkaline pH range [9]. This non-aqueous solvent enables experiments to be conducted in the absence of active residual water, ensuring that surface transformations are solely attributable to the properties of ammonia. From a fundamental perspective, the SC/ NH_3 Liq. interface introduces novel concepts that deviate from those established for aqueous electrolytes. Among III-V semiconductors InP or

GaP compounds exhibit unique electrochemical behavior when anodic processes are initiated [10,11]. This leads to a remarkable passivation phenomenon associated with the formation of an ultra-thin Polyphosphazene (PPP) film onto InP first [12–14]. Although the passivation mechanism is not yet fully understood, it appears to involve two consecutive steps: The initial anodic electrochemical dissolution of InP, which releases phosphorus (P^{3+}) and Indium (In^{3+}) cations into the solution. Subsequently, these phosphorus cations react with ammonia, leading to the chemical precipitation of a Polyphosphazene (PPP)-like film onto the InP surface. This process creates a superficial and complete covering network with a “P-N” skeleton structure, significantly altering the junction's electrochemical response. Studies of this phenomenon have recently focused on lightly doped n-type InP ($10^{15}/\text{cm}^3$). Using lightly doped InP allows passivation to occur exclusively through the consumption of photo-generated holes, facilitating a quantitative understanding of hole consumption and thereby enabling better control over PPP film formation [15]. XPS analyses further elucidate the

^{*} Corresponding author.

E-mail address: gianluca.visagli@uvsq.fr (G. Visagli).

<https://doi.org/10.1016/j.elecom.2025.107935>

Received 18 December 2024; Received in revised form 24 January 2025; Accepted 15 April 2025

Available online 15 April 2025

1388-2481/© 2025 The Authors. Published by Elsevier B.V. This is an open access article under the CC BY license (<http://creativecommons.org/licenses/by/4.0/>).

chemistry of the passivation film, revealing new specific N and P photo peaks and confirming the ultra-thin nature of the PPP film, as it shields the InP surface response. Electrochemical observations demonstrate the formation of the passivation layer, including a shift of more than 1 V in the flat-band potential, and the disappearance of the photopotential at V_{OC} [15,16]. The purpose of this paper is to elucidate these specific electrochemical behaviors using impedance measurements and cycle voltammetry.

2. Experimental

Indium phosphide (InP) wafers with an n-type doping concentration of 10^{15} cm^{-3} and a (100) crystallographic orientation, procured from InPact Electronic Materials, Ltd., are cleaved into square samples with an area of 0.1 cm^2 and a thickness of $350 \mu\text{m}$. Before passivation, these samples undergo chemo-mechanical polishing using a 2 % solution of Br_2 in methanol (CH_3OH), followed by an extensive rinse in high-purity methanol and subsequent drying using a nitrogen (N_2) stream. To remove any residual surface oxides, the samples are immersed briefly in a 2 M HCl solution immediately before experimentation and rinsed with ultra-pure H_2O [17,18]. For the electrochemical passivation process, NH_3 is condensed from electronic-grade gaseous ammonia supplied by Air Liquide. To improve the conductivity of the electrolyte, high-purity ammonium bromide (NH_4Br) at a concentration of 3.10^{-2} M (from Sigma Aldrich) is dissolved in the liquid ammonia to provide a constant pH given by NH_4Br full dissociated ion into NH_4^+ , the strongest acid in NH_3 Liq. [9]. A constant pH of 1.3 (referred to ammonia scale) prevents any variation in the flat band potential (V_{fb}) [19]. The electrochemical setup involves a conventional three-electrode configuration connected to a Parstat 2273 potentiostat, with a platinum counter-electrode and a silver reference electrode (SRE) [20] for potential measurement. The InP illumination is provided by an optical fiber immersed in a cryostat at -55°C where the electrochemical cell was placed. Interfacial impedance measurements are conducted at a frequency of 1.03 kHz with a scan rate of 5 mV/s. Mott–Schottky analysis was employed to gain deeper insights into the semiconductor properties of InP electrodes interfaced with liquid ammonia. Plotting the inverse square of the capacitance against the applied potential yielded the Mott–Schottky plot, the linearity in the Mott–Schottky plot indicates that the semiconductor is in the depletion regime, where majority carriers are depleted near the surface, forming a space-charge layer (SCL). From the slope of this linear portion, it is possible to determine the expected doping concentration of the InP electrodes. The intercept of the extrapolated line at $C^{-2} = 0$ corresponds to the flat band potential (V_{fb}), a critical parameter representing the potential at which no band bending and no space-charge region exists at the interface [21]. This intercept is obtained through mathematical extrapolation, as experimentally reaching V_{fb} is not possible due to the consistent presence of a band-bending at InP/electrolyte interface.

3. Results and discussion

The electrochemical behavior of indium phosphide (InP) in liquid ammonia was explored using cyclic voltammetry over a potential range from -0.5 V to $+2.0 \text{ V}$ versus the silver reference electrode (SRE) with a scan rate set at 20 mV/s . For lightly doped n-InP with a carrier concentration of 10^{15} cm^{-3} , the cyclic voltammogram recorded in the dark showed negligible anodic current throughout the entire potential range (Fig. 1). Under illumination with reduced light intensity (1 % of the reference flux, Φ_0). The reference flux corresponds to the maximum power output of the white light fiber optic source, SCHOTT KL 2500 LED. This light source allows precise beam power control by adjusting the output as a percentage of the maximum flux. The photocurrent onset was observed at $+0.2 \text{ V}$ vs. SRE during the initial anodic sweep. The steady-state photocurrent density reached approximately $4 \mu\text{A}\cdot\text{cm}^{-2}$, consistent with values reported in aqueous electrolytes under similar illumination conditions and in the dark no anodic current is observed

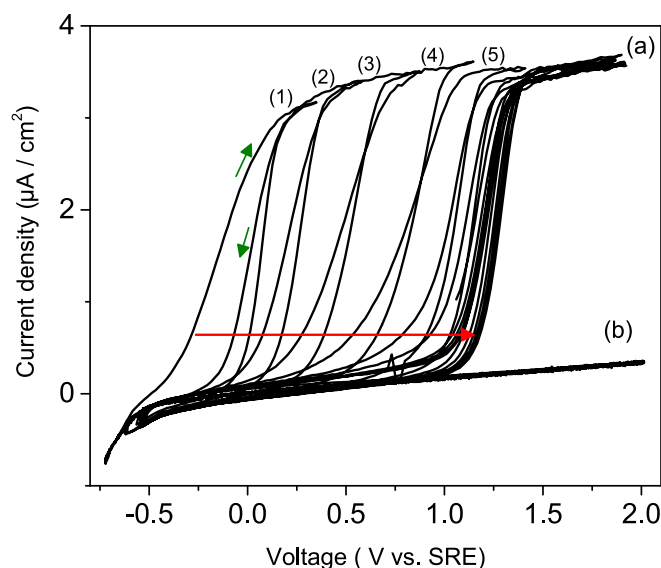


Fig. 1. Cyclic voltammetry of n-InP (10^{15} cm^{-3}) in NH_3 Liq. at 20 mV/s (NH_4Br , 3.10^{-2} M , at -55°C). (a) Anodic scans (from 1 to 5) under reduced light intensity (1 % Φ_0). (b) successive scans in the dark.

[22]. The photocurrent was directly proportional to light intensity, confirming the photoactivity of the n-InP electrode. Successive cyclic voltammograms were recorded by incrementally increasing the upper potential limit by about 150 mV. With each scan, a progressive positive shift in the onset potential for the photocurrent was noted. After multiple scans, the onset potential shifted from 0.2 V to 1.2 V vs. SRE. This shift of one volt remained stable even when the potential was swept up to $+2.0 \text{ V}$ vs. SRE under illumination. The photocurrent after the passivation, is still proportional to the incident flux intensity, accordingly to Gärtner's Law [23,24]. The gradual positive shift in the photopotential indicates the formation of a passivating layer at the InP/ NH_3 interface. This passivation phenomenon is attributed to the formation of a Polyphosphazene (PPP) film during the photoanodic treatment [12–15]. In lightly doped n-InP (10^{15} cm^{-3}), this process occurs primarily due to photogenerated holes, allowing precise control over the passivation and the anodic charge involved (0.5 mC/cm^2). According to the hypothesis that the anodic charge results only from InP dissolution through a six holes mechanism [25] an estimated thickness of the anodically dissolved InP monolayer is 0.3 nm. X-ray photoelectron spectroscopy (XPS) analyses confirmed the formation of the PPP film [14,15]. The spectra showed new peaks corresponding to phosphorus–nitrogen (P–N) bonds, indicative of the PPP structure. All over the surface, the constant attenuation of InP substrate signals observed in the XPS spectra indicates that the Polyphosphazene (PPP) film formed is homogeneous ultra-thin, yet significantly modifies the interface's surface chemistry and electronic properties. Moreover, the tiny amount of charge used during the passivation process suggests that only a few monolayers of InP were dissolved, confirming that the resulting PPP film is, indeed, thin.

3.1. Mott-Schottky plot shift due to PPP

The formation of the PPP film has significant implications for the electrochemical properties of the InP/ NH_3 interface. Mott-Schottky plots were acquired to analyze changes in the flat-band potential (V_{fb}) before and after passivation. The flat-band potential is a critical parameter indicating the potential at which the bands in the semiconductor are flat, and there is no space charge region [4,21]. In the unpassivated undoped n-InP, the Mott–Schottky plot exhibits a linear relationship, and V_{fb} determined from the intercept is -0.7 V vs. SRE. The slope of the linear portion is coherent with the expected doping level. The open-circuit

potential (V_{OCP}) was found to be approximately -0.2 V vs SRE (Fig. 2). At this V_{OCP} , the semiconductor is in a depletion regime because the flat-band potential is more negative than the V_{OCP} ($V_{\text{OCP}} > V_{\text{fb}}$) corresponding to a positive band-bending ($V_{\text{OCP}} - V_{\text{fb}}$) of $+500$ mV. Importantly, during this regime, the total capacitance is predominantly due to the semiconductor's capacitance, as the Helmholtz layer capacitance is much larger [26] and, being in series, contributes negligibly to the overall capacitance (Eq. 1).

$$\frac{1}{C_{\text{tot}}} = \frac{1}{C_{\text{SC}}} \quad (1)$$

After passivation, a significant positive shift in V_{fb} was observed (from -0.7 V to $+0.2$ V vs. SRE), as shown in Fig. 2. The V_{fb} shifted to more positive values, and the V_{OCP} of the passivated electrode was measured at approximately -0.10 V vs SRE. In this case, the semiconductor is in an accumulation regime at the V_{OCP} because the flat-band potential is now more positive than the V_{OCP} ($V_{\text{fb}} > V_{\text{OCP}}$) corresponding to a negative band-bending of -300 mV. In the accumulation regime, the surface is enriched by majority carriers (electrons).

The formation of the Polyphosphazene (PPP) film on the InP surface has significantly changed the electrochemical properties of the InP/ NH_3 interface. The shift in the V_{fb} value indicates that a more positive potential is required to achieve flat-band conditions in the passivated electrode as a result of strong chemical and electrical modifications at the passivated interface. On a passivated interface, from V_{OCP} to lower potentials, the semiconductor is in an accumulation regime, therefore electrons accumulate at the surface. The electrical charge becomes negative at the semiconductor side. This new interfacial configuration is consistent with the hypothesis that the PPP film is positively charged and that this influences the band bending in the semiconductor. In fact, it is possible to assume that the semiconductor changes its band-bending configuration at the V_{OCP} (from depletion to accumulation) to balance the positive charges of the PPP film and, therefore enhancing a capacitive behavior at InP/PPP interface. The positive charge can result from a combination of two factors. The first one can imply the hyperpolarizability of the P–N bond in the PPP film [27] which can act as a dipole. The second aspect is the interaction of PPP film with NH_3 Liq. acting as a strong polarizable solvent [9]. Understanding this shift from depletion to accumulation is crucial because it fundamentally changes the charge distribution and electric field at the semiconductor interface, impacting the device's photoelectrochemical behavior. Starting from an accumulation regime, on a InP/PPP interface, it is necessary to polarize

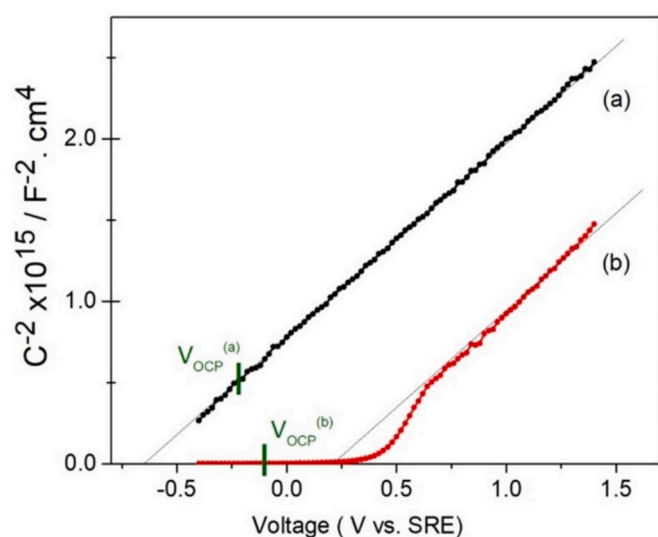


Fig. 2. Mott–Schottky plots of n-InP in NH_3 Liq. (NH_4Br , 3.10^{-2} M, at -55 °C), before (a) and after passivation (b) with PPP film.

1 V more than on a pristine InP interface for reaching again a depletion regime inside the semiconductor to allow photogenerated holes collection at the interface, as it is shown in the Fig. 1.

3.2. Capacitive-voltage measurements

Capacitance-voltage (C–V) measurements were performed to investigate this charge distribution. Fig. 3 illustrates the C–V curves before and after passivation. In the unpassivated state, the capacitance varies with potential, reflecting the changes in the space charge region of the semiconductor, the remarkable increase that can be seen around -0.6 V vs. SRE is due to faradic charge from protons reduction. After passivation, a substantial change in the C–V curve happens. A plateau between -0.2 V and -0.6 V vs. SRE is now present, where the capacitance remains constant over 400 mV despite changes in applied potential. This behavior was found in all of the samples and tends to be very reproducible, the mean value of the plateau is $1.10^{-6} \pm 0.2 \times 10^{-6}$ F cm^{-2} . This capacitance represents the combined contribution of the PPP film and the Helmholtz layer at the interface. However, we can confidently exclude the Helmholtz layer as the primary contributor to the measured capacitance for several reasons. Firstly, the Helmholtz capacitance typically varies with potential and does not exhibit a constant value over a wide potential range usually not extending beyond 50 mV [26]. In contrast, our observations show a consistent capacitance over a much broader potential range, which is characteristic of a real capacitor rather than the Helmholtz layer. Secondly, knowing that the viscosity of NH_3 Liq. is four times lower at -33 °C than water's at 25 °C [9], we can assume that the Helmholtz capacitance in NH_3 Liq. is on the order of 1×10^{-5} F cm^{-2} , which is significantly different from the capacitance values observed in our measurements. This disparity in magnitude further supports the conclusion that the Helmholtz layer's contribution is negligible compared to that of the PPP film.

Another typical capacitor behavior was observed during the study of InP/PPP interface. The provided cyclic voltammogram (Fig. 4) illustrates the electrochemical response of the InP/PPP system under various scan rates. In the potential range corresponding to the formation of the PPP passivation layer, the interface demonstrates clear capacitive behavior with charge and discharge behavior. This is particularly evident from the proportionality between the current and the scan rate, which is indicative of a charging and discharging current in a capacitor-like interface. In the capacitive region, the relationship between the current (I) and the scan rate (v) is given by the capacitive current Eq.

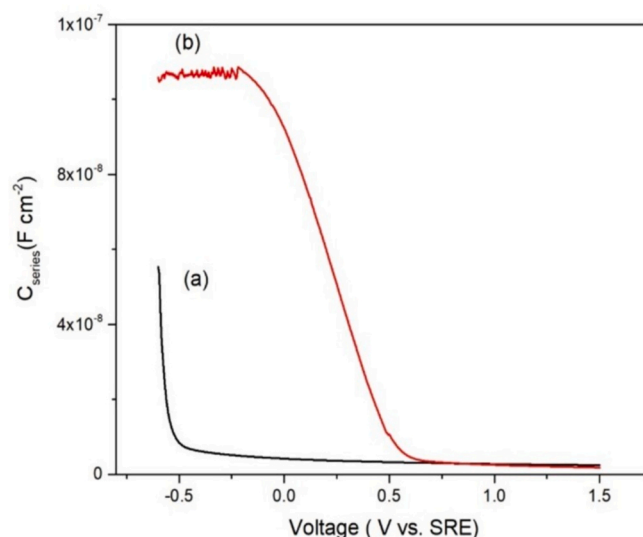


Fig. 3. Capacitance–voltage (C–V) curves of n-InP in NH_3 Liq. (NH_4Br , 3.10^{-2} M, at -55 °C) before (a) and after (b) passivation with PPP film.

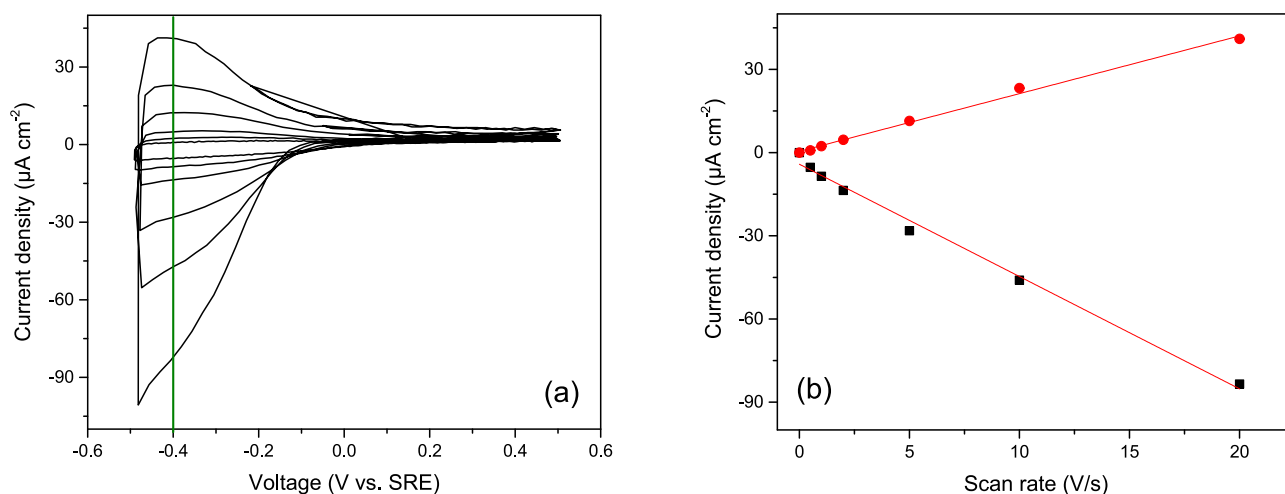


Fig. 4. (a) Cyclic voltammogram of InP/PPP interface in NH₃ Liq. (NH₄Br, 3.10⁻² M, at -55 °C), showing capacitive behavior proportional to the scan rate (0.5 V/s, 1 V/s, 2 V/s, 5 V/s, 10 V/s, 20 V/s). (b) Linear fit of the current density at -0.4 V/SRE, as a function of the scan rate.

[26] (Eq. 2).

$$i_c = \nu C_d + \left[\left(\frac{E_i}{R_s} - \nu C_d \right) \exp\left(\frac{-t}{R_s C_d}\right) \right] \quad (2)$$

When a capacitor is subject to a varying voltage over time, the current can be divided into two main components, a transient current (i_{trans}) and a steady-state current (i_{perm}). After these considerations, the total current in a capacitor can be written as shown in Eq. 3.

$$\dot{i}(t) = i_{trans}(t) + \dot{i}_{perm} \quad (3)$$

In cyclic voltammetry, the capacitive current measured during the experiment is predominantly in the steady-state regime. This occurs because the timescale of the voltage scan ensures that the transient effects become negligible relative to the steady-state current. For time-varying voltage (V) (e.g., scan rate), the current will directly follow the variations in $V(t)$. As shown in Fig. 4, this principle was applied in InP/PPP interface, the linearity of the data points in the inset of Fig. 4 shows a high correlation ($R^2 = 0.998$), giving a value for the capacitance of 1.9 10⁻⁶ F cm⁻². This value is coherent with the one empirically found with C–V curves (Fig. 3). It is therefore possible to assert that the InP/PPP interface behaves like a capacitor, with the current directly proportional to the scan rate. The slope of the linear regression line obtained from the graph represents the system's capacitance.

On passivated InP, for applied potentials (V_{App}) between -0.2 V and -0.6 V vs. SRE (corresponding with the plateau in the C–V curves, Fig. 3), the semiconductor is in an accumulation regime, ($V_{App} < V_{fb}$). Importantly, in this regime, the semiconductor capacitance (C_{sc}) is neglectable [28]. Since the same range of potential was explored, the Helmholtz layer capacitance is still negligible (Fig. 2). Therefore, total capacitance is predominantly due to the PPP capacitance, as shown in Eq. 4.

$$\frac{1}{C_{tot}} = \frac{1}{C_{ppp}} \quad (4)$$

The constant capacitance observed in the plateau region suggests that the PPP film acts as a dielectric layer with a fixed capacitance. This behavior is characteristic of a parallel-plate capacitor, where the capacitance is shown in Eq. 5 [26].

$$C_{ppp} = \frac{\epsilon_r \epsilon_0 A}{d} \quad (5)$$

The ϵ_r represents the relative dielectric constant of the PPP film, ϵ_0 the vacuum permittivity, A the area of the electrode, and d the thickness of the PPP film.

3.3. Relative permittivity coefficient calculation

The calculation of the relative permittivity (ϵ_r) of the Polyphosphazene (PPP) film was conducted using the average plateau capacitance value (C) obtained from the capacitance-voltage (C–V) curves. The thickness (d) of the PPP film was estimated based on literature data by considering the cumulative bond lengths of the three main chemical bonds in the PPP structure (“In-P”, “P-N” and “N-H”) [27,29,30]. This spatial configuration of PPP has been recently confirmed by coupling XPS and p-ARXPS techniques [34]. This approach yielded an estimated film thickness of approximately 0.5 nm. The area of the electrode (A) used in the measurements was known from the sample preparation, being 0.1 cm². We assume that there was no significant development of surface area due to the passivation, as the film is nanometrically thin. Utilizing the vacuum permittivity constant ($\epsilon_0 = 8.854 \times 10^{-12}$ F/m), we calculated the relative permittivity (ϵ_r) of the PPP film to be approximately 6.9. This value aligns well with typical permittivity values for polymeric materials known for their good insulating capabilities [31–33]. The presence of a relatively high permittivity confirms that the PPP film acts as an effective dielectric layer, capable of stabilizing the charge accumulated at the interface between the film and the InP surface. This dielectric behavior is crucial for the observed capacitive properties of the system. This understanding is essential for accurately interpreting the electrochemical behavior of the passivated InP electrode and for optimizing the design of efficient photoanodes in photoelectrochemical applications.

4. Conclusion

The formation of a positively charged Polyphosphazene (PPP) film on lightly doped n-InP in liquid ammonia significantly modifies the electrochemical properties of the semiconductor/liquid interface. Before passivation, the semiconductor was in depletion configuration at the V_{OCB} , however, once passivated, at the V_{OCB} the semiconductor is in accumulation regime. The PPP film introduces capacitive behavior due to the interaction between its positive charges and the accumulated electrons at the semiconductor surface. This behavior was demonstrated through cyclic voltammetry at various scan rates, where the current was shown to be directly proportional to the scan rate, confirming a capacitive charging mechanism. Capacitance–voltage measurements further supported the formation of a stable capacitor-like structure, with a constant capacitance indicative of a fixed dielectric layer formed by the PPP film. The capacitive charging equation applies to this region, confirming the role of the PPP film as an effective dielectric. The

capacitance obtained in this region was further used to calculate the relative dielectric constant (ϵ_r) of the PPP layer, which was found to be approximately 6.9. This value is consistent with that of polymeric materials with good insulating capabilities, confirming the effective role of the PPP film as a dielectric layer. The PPP film effectively separates charges across its thickness, storing energy in the electric field established between the positively charged film and the semiconductor's negative charges. The insights gained here contribute to a deeper understanding of semiconductor passivation mechanisms in non-aqueous environments and demonstrate the importance of capacitive effects in modifying and enhancing the electrochemical response of semiconductor interfaces.

CRedit authorship contribution statement

Gianluca Visagli: Writing – review & editing, Writing – original draft, Investigation, Data curation, Conceptualization. **Arnaud Etcheberry:** Writing – review & editing, Writing – original draft, Validation, Supervision, Resources, Investigation. **Anne-Marie Gonçalves:** Writing – review & editing, Writing – original draft, Validation, Supervision, Resources, Project administration, Methodology, Conceptualization.

Declaration of competing interest

The authors declare that they have no known competing financial interests or personal relationships that could have appeared to influence the work reported in this paper.

Data availability

Data will be made available on request.

References

- [1] H. Gerischer, *Semiconductor Electrode Reactions*, in *Advances in Electrochemistry and Electrochemical Engineering*, Interscience, New York, 1965.
- [2] C.G.B. Garrett, *Semiconductor Aspects of a Semiconductor Electrode*, in the *Electrochemistry of Semiconductors*, Academic Press, London and New York, 1962.
- [3] R. Memming, *Processes at Semiconductor Electrodes*, in *Comprehensive Treatise of Electrochemistry*, Plenum Press, New York, 1983.
- [4] W. Schmickler, S. Roy Morrison, *Electrochemistry at semiconductor and oxidized metal electrodes*. Plenum press, New York, London, Ber. Bunsenges. Phys. Chem. 85 (1981) (1980) 621–622, <https://doi.org/10.1002/bbpc.19810850728>.
- [5] F.A. Uribe, A.J. Bard, *Electrochemistry in liquid ammonia*. 5. Electroreduction of oxygen, *Inorg. Chem.* 21 (1982) 3160–3163, <https://doi.org/10.1021/ic00138a048>.
- [6] R.E. Malpas, K. Itaya, A.J. Bard, *Semiconductor electrodes*. 20. Photogeneration of solvated electrons on p-type gallium arsenide electrodes in liquid ammonia, *J. Am. Chem. Soc.* 101 (1979) 2535–2537, <https://doi.org/10.1021/ja00504a006>.
- [7] R.E. Malpas, K. Itaya, A.J. Bard, *Semiconductor electrodes*. 32. n- and p-gallium arsenide n- and p-silicon, and n-titanium dioxide in liquid ammonia, *J. Am. Chem. Soc.* 103 (1981) 1622–1627, <https://doi.org/10.1021/ja00397a003>.
- [8] M. Herlem, D. Guyomard, C. Mathieu, J. Belloni, J.L. Sculfort, Behavior of n-type and p-type silicon in anhydrous liquid ammonia. The solvated electron generation: a supra-band-edge reaction, *J. Phys. Chem.* 88 (1984) 3826–3833, <https://doi.org/10.1021/j150661a028>.
- [9] J. Jander, *Chemie in Wasserfreiem flüssigem Ammoniak: Chemistry in Anhydrous Liquid ammonia*, Vieweg & Sohn, 1999.
- [10] A.-M. Gonçalves, C. Mathieu, A. Etcheberry, Electrochemical comparisons between GaAs and InP in liquid ammonia regarding the anodic passivation process, *J. Electrochem. Soc.* 159 (2012), <https://doi.org/10.1149/2.074202jes>.
- [11] A.-M. Gonçalves, C. Mathieu, M. Herlem, A. Etcheberry, A striking anodic behaviour of p-GaAs semiconductor in acidic liquid ammonia (223K), *Electrochim. Acta* 46 (2001) 2835–2841, [https://doi.org/10.1016/S0013-4686\(01\)00498-4](https://doi.org/10.1016/S0013-4686(01)00498-4).
- [12] A.-M. Gonçalves, O. Seitz, A. Eb, C. Mathieu, M. Herlem, A. Etcheberry, A Significant Anodic Passivation of N and P-InP Surfaces in Liquid ammonia: First Evidence of Stable Phosphorus-Nitrogen Bonds, *ECS Trans.* 2007, pp. 461–468, <https://doi.org/10.1149/1.2731214>.
- [13] A.-M. Gonçalves, O. Seitz, C. Mathieu, M. Herlem, A. Etcheberry, First evidence of stable P-N bonds after anodic treatment of InP in liquid ammonia: a new III-V material passivation route, *Electrochem. Commun.* 10 (2008) 225–228, <https://doi.org/10.1016/j.elecom.2007.11.018>.
- [14] A.-M. Gonçalves, N. Mézailles, C. Mathieu, P. Le Floch, A. Etcheberry, Fully protective yet functionalizable monolayer on InP, *Chem. Mater.* 22 (2010) 3114–3120, <https://doi.org/10.1021/cm100035a>.
- [15] A.M. Gonçalves, G. Visagli, C.P. Rakotoarimanana, C. Njel, M. Frégnaux, Photoelectrochemical passivation of undoped n-InP by ultra-thin polyphosphazene film: towards a perfect photoanode? *Electrochim. Acta* 470 (2023) 143326 <https://doi.org/10.1016/j.electacta.2023.143326>.
- [16] C. Njel, I. Bakas, D. Aureau, A.-M. Gonçalves, A. Etcheberry, Photoelectrochemical studies and capacitance measurements during the nitride passivation of InP in liquid ammonia (–55°C), *ECS Trans.* (2015) 83–88, <https://doi.org/10.1149/O6606.0083ecst>.
- [17] N. Simon, N.C. Quach, A.M. Gonçalves, A. Etcheberry, Growth of anodic oxides on n-InP studied by electrochemical methods and surface analyses, *J. Electrochem. Soc.* 154 (2007), <https://doi.org/10.1149/1.2709504>.
- [18] S. Béchu, D. Aureau, A. Etcheberry, Surface evolution of InP substrates at the frontier between deoxidation and dissolution in HCl solutions, *Surf. Interface Anal.* 55 (2023) 515–520, <https://doi.org/10.1002/sia.7152>.
- [19] A.-M. Gonçalves, C. Mathieu, M. Herlem, A. Etcheberry, The pH response of the InP/liquid ammonia interface at 223 K: a pure nernstian behavior, *Electrochim. Acta* 55 (2010) 7413–7418, <https://doi.org/10.1016/j.electacta.2010.07.001>.
- [20] A. Etcheberry, A.-M. Gonçalves, C. Mathieu, M. Herlem, Cathodic decomposition of n-InP during hydrogen evolution in liquid ammonia, *J. Electrochem. Soc.* 144 (1997) 928–935, <https://doi.org/10.1149/1.1837509>.
- [21] P. Blood, Capacitance-voltage profiling and the characterisation of III-V semiconductors using electrolyte barriers, *Semicond. Sci. Technol.* 1 (1986) 7–27, <https://doi.org/10.1088/0268-1242/1/1/002>.
- [22] O. Seitz, C. Mathieu, A.-M. Gonçalves, M. Herlem, A. Etcheberry, Interfacial anodic behaviors of n- and p-GaAs semiconductors in liquid ammonia at 223 K, *J. Electrochem. Soc.* 150 (2003), <https://doi.org/10.1149/1.1603249>.
- [23] W.W. Gärtner, Depletion-layer Photoeffects in semiconductors, *Phys. Rev.* 116 (1959) 84–87, <https://doi.org/10.1103/PhysRev.116.84>.
- [24] P. Lemasson, A. Etcheberry, J. Gautron, Analysis of photocurrents at the semiconductor–electrolyte junction, *Electrochim. Acta* 27 (1982) 607–614, [https://doi.org/10.1016/0013-4686\(82\)85048-2](https://doi.org/10.1016/0013-4686(82)85048-2).
- [25] O. Seitz, C. Mathieu, A.-M. Gonçalves, M. Herlem, A. Etcheberry, Interfacial anodic behaviors of n- and p-GaAs semiconductors in liquid ammonia at 223 K, *J. Electrochem. Soc.* 150 (2003), <https://doi.org/10.1149/1.1603249>.
- [26] A.J. Bard, L.R. Faulkner, *Electrochemical Methods: Fundamentals and Applications*, Wiley, John Wiley & Sons, New York, 2001.
- [27] L. Kapička, P. Kubáček, P. Holub, Bonding and aromaticity of cyclic phosphazenes viewed as interaction of Dnh fragments, *J. Mol. Struct. (THEOCHEM)* 820 (2007) 148–158, <https://doi.org/10.1016/j.theochem.2007.06.022>.
- [28] P. Allongue, J.-N. Chazalviel, C. Henry de Villeneuve, F. Ozanam, Analysis of Capacitance Potential measurements at the silicon–electrolyte interface revisited, *J. Phys. Chem. C* 111 (2007) 5497–5499, <https://doi.org/10.1021/jp068614z>.
- [29] J.P. Rino, P.S. Branício, Structural phase transformations in InP under pressure: a molecular-dynamics study, *Phys. Status Solidi B* 244 (2007) 239–243, <https://doi.org/10.1002/pssb.200672550>.
- [30] J. Demaison, J. Liévin, A.G. Császár, C. Gutle, Equilibrium structure and torsional barrier of BH₃NH₃, *J. Phys. Chem. A* 112 (2008) 4477–4482, <https://doi.org/10.1021/jp710630j>.
- [31] S. Uzaki, K. Adachi, T. Kotaka, Multiple dielectric relaxations in solid Polyorganophosphazenes, *Polym. J.* 20 (1988) 221–229, <https://doi.org/10.1021/polymj.20.221>.
- [32] K. Moriya, Y. Nishibe, S. Yano, Dielectric properties of poly[bis(trifluoroethoxy) phosphazene] and poly[bis(m-methylphenoxy) phosphazene], *Macromol. Chem. Phys.* 195 (1994) 713–721, <https://doi.org/10.1002/macp.1994.021950228>.
- [33] G. Allen, C.J. Lewis, S.M. Todd, Polyphosphazenes: Part 2. Characterization, *Polymer (Guildf)* 11 (1970) 44–60, [https://doi.org/10.1016/0032-3861\(70\)90061-3](https://doi.org/10.1016/0032-3861(70)90061-3).
- [34] G. Visagli, A. Etcheberry, M. Frégnaux, A.M. Gonçalves, Surface and Interface Analysis 57 (5) (2025) 327–333, <https://doi.org/10.1002/sia.7389>.